On-chip full-field test engine for photonic integrated devices based on optical frequency domain reflectometry technique

(Student paper)

Luis A. Bru,[1] Daniel Pastor,[1] Bernardo Gargallo,[2] David Doménech,[2]
Carlos Domínguez,[3] and Pascual Muñoz[1]
[1]*Universitat Politècnica de València, c/ Camino de Vera s/n - 46021 Valencia - Spain*
pascual.munoz@upv.es
[2]*VLC Photonics S.L., c/ Camino de Vera s/n - 46021 Valencia - Spain*
[3]*Institut de Microelectrònica de Barcelona CNM-CSIC - 08193 Cerdanyola del Vallès - Barcelona - Spain*

ABSTRACT

In this work we report on a fully integrated photonic chip test structure, providing optical amplitude and phase, frequency and time domain resolution for on-chip devices under test. The structure is based on optical frequency domain reflectometry, and compared to previous approaches, and by suitable design, it allows for retrieving full-field information on the device under test through a single pair of input/output optical ports, with inherent waveguide dispersion de-embedding. As a proof of concept, an experimental demonstration is performed for an arrayed waveguide grating fabricated on a silicon nitride photonic integration platform.

Keywords: optical frequency domain reflectometry, integrated test device, dispersion compensation, interferometry, arrayed waveguide grating, silicon nitride.

1 INTRODUCTION

In the world of modern integrated photonics, devices and circuits are getting more and more complex and posing increasing demands to characterization. Hence, optical frequency domain reflectometry (OFDR) [1]–[3] comes up as a very convenient technique due to its relatively simple implementation, still holding a good balance between accuracy, sensitivity, length range and time/spatial resolution [3]. Recently, approaches involving the integration on-chip of interferometric parts have appeared in the literature [4]–[6], showing improvements in terms of test setup compactness. In our previous work [5], we intendedly proposed to integrate OFDR Mach-Zehnder interferometers (MZI) as such (IOFDR), with the added advantages of extended versatility (holding any chip coupling strategy, accurate design of interferometer delays, as well as reflectometry and transmission arrangements). Remarkably, the approach inherently incorporates a (universal) dispersion de-embedding mechanism as well, something demonstrated for an arrayed waveguide grating (AWG) as a device under test (DUT). An important drawback in IOFDR is the simultaneous detection from two optical ports, something specially cumbersome on passive integrated optics having to employ a fiber array. In this work, we propose a device addressing this issue, by making use of a modified OFDR-based structure, but still preserving characteristics from our previous approach. We shall discuss this matter in section 2, to then show the experimental proof-of-concept in section 3, and finally draw our conclusions in section 4.

2 INTEGRATED TEST DEVICE

OFDR is a well-known homodyne interferometric technique providing both amplitude and phase, frequency and time domain resolution. It draws on two interferometers (typically MZI) to get interferogram data (containing amplitude and phase spectral information of the DUT) and correcting signal for proper triggering (TRIG) and therefore linearization of the optical frequency scan, indispensable to properly apply inverse fast Fourier transform (IFFT) algorithm and obtain time domain response.

The simultaneous detection of two optical ports in OFDR technique is quite an inconvenience from a practical point of view, when the signals have to be gathered from integrated waveguides on passive chip technologies, which require a fiber array as it happens for our IOFDR approach in [5]. A more straightforward single input/output detection arrangement is always preferable, so an advance interferometric system configuration is required, in order to be able to collect all the information of both conventional interferometers. In the test engine we propose hereby, these conditions are met with a 3-way interferometer (3-MZI), conveniently involving a single pair of input/ouput optical ports, and thus enabling single optical detection. An sketch of the proposed test structure is included in Fig. 1(a), where the lengths for the corresponding 3 different arms are L_1, L_2 and L_3 (being $L_1 < L_2 < L_3$, by convention). The 3-MZI can be conceived to be composed by 3 conventional 2-way interferometers which path length differences (PLDs) correspond to the following combinations of designed lengths:

$$\Delta L_{\text{DUT}} = L_2 - L_1,\ \Delta L_{\text{TRIG}} = L_3 - L_2 \text{ and } \Delta L_{\text{ADD}} = L_3 - L_1, \quad (1)$$

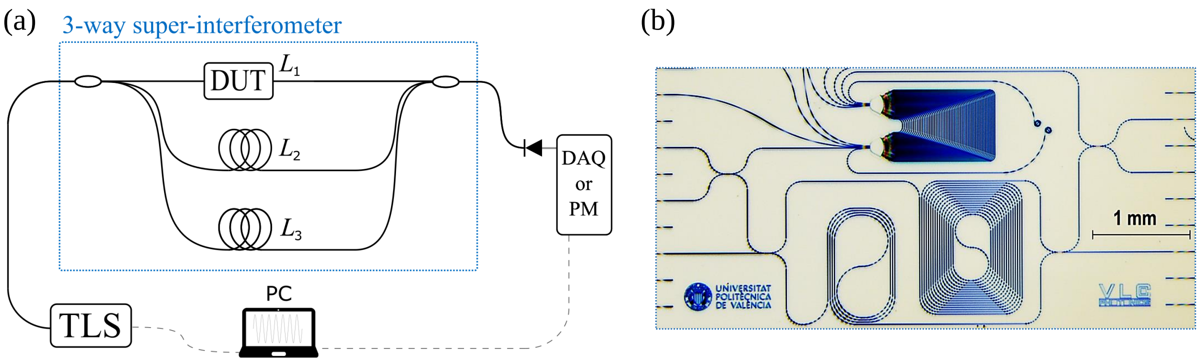

Figure 1. (a) A sketch of the proposed device and setup. In (b) a microscope photograph of the fabricated device.

i.e. the two firsts are for the DUT and TRIG interferograms as already reported, and an additional one (ADD) is incorporated. At this point, let us note that 3-MZI interferogram is not properly linearized, so it contains all the 'raw' information about interferograms including phase scanning error and dispersion. In spite of it, IFFT can be applied anyhow and identify the desired $\Delta L_{\text{DUT}}, \Delta L_{\text{TRIG}}$ contributions in the impulse domain. Then, by individually slicing contributions can be filtered, and by applying FFT to them, the interferograms are separately recovered. This in turn requires an additional processing step, and where PLDs have to be carefully designed: given a ΔL_{DUT}, applying the Nyquist criterion results into $\Delta L_{\text{TRIG}} \geq 2\Delta L_{\text{DUT}}$ (e.g. $\Delta L_{\text{TRIG}} = 4\Delta L_{\text{DUT}}$ places DUT in the center of the (semi) time window) and the third contribution ΔL_{ADD} will appear at a 'distance' ΔL_{DUT} away from ΔL_{TRIG}, so ΔL_{DUT} (and hence ΔL_{TRIG}) must account for it to prevent overlapping in the impulse domain.

Further, the proposed test device remarkably incorporates an inherent dispersion de-embedding system as in IOFDR [5]. The same waveguides for the involved MZIs and the DUT are influenced by the same dispersion phase chirp in the corresponding interferograms, in such a way that they are cancelled in the linearization process. Dispersion-free resolved time domain response is particularly convenient in the case of integrated devices, for which maximizing spatial resolution of the system (ultimately given by scanning span [2]) is crucial to indentify specially nearby events taking place in waveguides which very oftenly present high dispersion.

3 EXPERIMENTAL RESULTS

The employed setup for the measurements consists of simply introducing light in and out of the chip, as shown in Fig. 1(a): a tunable laser source (TLS) provides a continuous scanning signal at speed $v = 20$ nm/s and 80 nm span centered @1550 nm feeding the chip by horizontal coupling through one of the available inputs. Light goes over the 3 different paths, as depicted in Fig. 1(b) (Si_3N_4 waveguides of 280×1000 nm film height and width and group index $n_g^{\text{TE}} = 1.86$ for the TE mode [7]), splitting in amplitude by 2×2 multimode interferometers (MMI) and finally being combined the same way and collected at one of the outputs. The resulting signal is photodetected by a PIN (InGaAs) photodiode and acquired by a data acquisition card (DAQ) (at a rate of 100 kS/s) to be stored and post-processed. In Fig. 2(a) the generated 3-MZI interferogram is plotted: as described in section 2, IFFT algorithm is performed to the raw data so that desired contributions of the conventional interferograms, which are placed where designed (physical PLDs of $\Delta L_{\text{DUT}} = 1$ and $\Delta L_{\text{TRIG}} = 3.5$ cm), can be filtered back by FFT to the frequency domain. The result of this double transformation operation

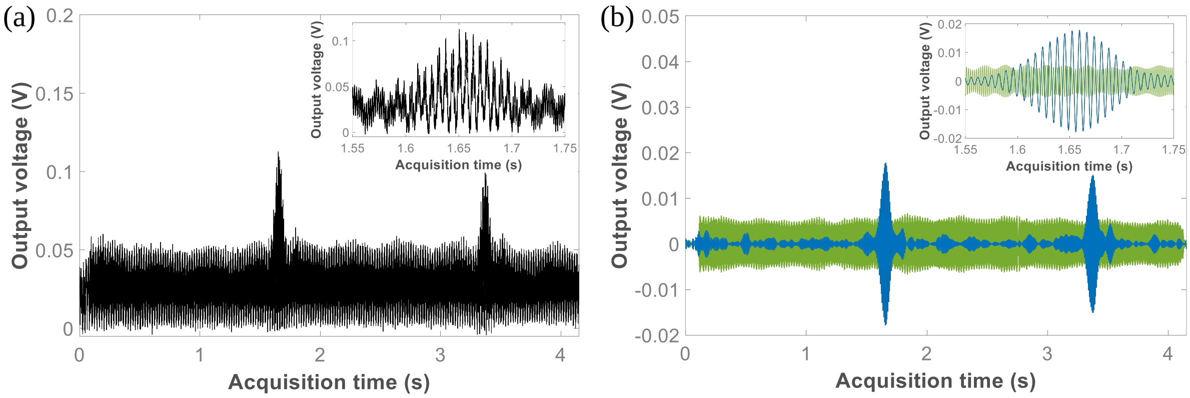

Figure 2. (a) The 3-MZI interferogram from where conventional DUT and TRIG interferograms are filtered and shown in (b). In the insets, a zoomed view of the first strong peak around 1.65 s is provided.

is shown in Fig. 2(b), in blue and green for the DUT and the TRIG, respectively.

From this point, we proceed as usual for the OFDR technique. After properly linearizing the DUT interferogram with the TRIG data, the time domain response for the AWG is retrieved by an IFFT, and plotted in Fig. 3(a). The AWG was designed with 59 waveguides in the array and a free spectral range (FSR) of 32 nm (4 THz), same as in [5] and manufactured in the silicon nitride process of CNM-VLC [8]. Most of the waveguides can be perfectly identified, with a time separation of 0.24 ps ($\sim 38\,\mu$m) as expected. This is possible because of the dispersion de-embedding of on-chip OFDR. Otherwise with the existing waveguide dispersion of $D = -1.32$ ps/nm·m (see [7]), the associated temporal broadening of $\Delta T = 0.95$ ps ($\sim 153\,\mu$m) corresponds to almost 4 times the actual peak spacing, and peak visibility would be blurred. The AWG contributions in time

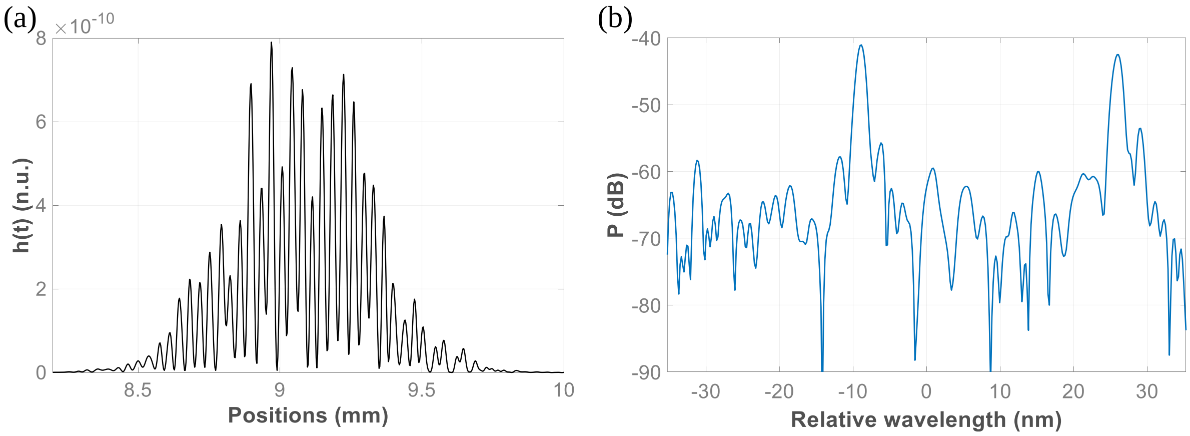

Figure 3. (a) Time domain response of the AWG, where the compensated different contribution peaks for the waveguides of the array can be perfectly distinguished. In (b), the frequency domain spectral amplitude of the AWG obtained by bandpass filtering.

domain, or position as depicted in Fig. 3(a), are extracted by slicing at the proper time/space range (besides removing detection noise and spurious time events on the chip) and the FFT is applied again to obtain the AWG spectral response in Fig. 3(b).

4 CONCLUSIONS

We have reported on a novel integrated test structure based on OFDR technique, inheriting all the capabilities from our previous work device, the IOFDR in [5] (remarkably, the mentioned dispersion compensation mechanism). The device is able to work in a single pair input/output detection arrangement so suitable in integrated optics, by translating part of the complexity to the post processing. Promising experimental results have been also reported, demonstrating the validity of the technique through the proposed test structure, by testing a designed AWG as a DUT on a silicon nitride platform. The dispersion-compensated time domain response of the AWG has been successfully resolved as expected, from which the spectral response of the AWG can be reconstructed as well.

ACKNOWLEDGMENT

The authors acknowledge financial support through projects, TEC2015-69787-REDT PIC4TB, TEC2016-80385-P SINXPECT, TEC2014-54449-C3-1-R BIOSENSLOC and GVA PROMETEO 2017/103. L.A.B. also acknowledges PTA2015-11309-I.

REFERENCES

[1] W. Eickhoff and R. Ulrich, "Optical frequency domain reflectometry in single-mode fiber," Appl. Phys. Lett. 39(9), pp. 693-695, 1981.

[2] U. Glombitza and E. Brinkmeyer, "Coherent frequency-domain reflectometry for characterization of single-mode integrated-optical waveguides," J. Lightwave Technol. 11, pp. 1377-1384, 1993.

[3] B. J. Soller, D. K. Gifford, M. S. Wolfe and M. E. Froggatt, "High resolution optical frequency domain reflectometry for characterization of components and assemblies," Opt. Express 13, pp. 666-674, 2005.

[4] D. Melati, "A design kit perspective in InP-based photonic integrated circuits," Ph.D. Thesis, Polytechnic University of Milan, 2014.

[5] L. A. Bru et al., "Fully Integrated Optical Frequency Domain Reflectometry," in proceedings of European Conference on Integrated Optics (ECIO) 2017, paper M3.5 (April 2017).

[6] D. Zhao, D. Pustakhod, K. Williams, and X. Leijtens, "High resolution optical frequency domain reflectometry for analyzing intra-chip reflections," IEEE Photon. Technol. Lett., vol. 29, no. 16, pp. 1379–1382, 2017.

[7] G. Micó et al., "Silicon nitride photonics: from visible to mid-infrared wavelengths," in proceedings of SPIE Photonics West 2018: Silicon Photonics XIII, pp. 10537-9, 2018.

[8] Silicon Nitride Photonic Integration Platform, http://www.imb-cnm.csic.es/index.php/en/clean-room/silicon-nitride-technology